INTERNATIONAL JOURNAL OF AUTOMOTIVE AND MECHANICAL ENGINEERING (IJAME)
ISSN: 2229-8649 e-ISSN: 2180-1606
VOL. 20, ISSUE 1, 2023, 10285 – 10297
DOI: https://doi.org/10.15282/ijame.20.1.2023.10.0795

ORIGINAL ARTICLE

Artificial Neural Network-Based Fault Detection System with Residual Analysis Approach on Centrifugal Pump: A Case Study

Katherin Indriawati[1,*], Gabriel Fransisco Yugoputra[1], Noviarizqoh Nurul Habibah[1], and Risma Yudhanto[2]

[1]Department of Engineering Physics, Sepuluh Nopember Institute of Technology, 60111 Indonesia
[2]Saka Indonesia Pangkah Limited, 61151 Indonesia

ABSTRACT – Centrifugal pump is an instrument that is widely used in industry and has become the main driving component. A detection system is often needed to prevent damage to these pumps because they can interfere with the overall system performance. Therefore, this study discussed the development of a fault detection system for two centrifugal pump units, namely the Medium Pressure Oil Pump (MPOP) and the Water Injection Pump (WIP). In detecting the operating conditions of the pump, it was used a residual feature extraction technique in the time domain with a statistical approach. Residual was generated by using three sub-systems of a pumping system. Each sub-system was modeled using an artificial neural network with feedforward-back propagation architecture. Based on the feature values, the classifier was designed to classify pump conditions. Then the proposed fault detection system was applied in a condition monitoring system scheme. The test results (using data from the field) show that the fault detection system has an accuracy of 91.67% for MPOP and 94.8% for WIP cases. Meanwhile, the fault detection system has an accuracy above 99% during online monitoring simulations.

ARTICLE HISTORY
Received: 09th Jan 2022
Revised: 29th Dec 2022
Accepted: 15th Feb 2023
Published: 07th Apr 2023

KEYWORDS
Centrifugal pump;
Classifier;
Data bank;
Artificial neural network;
Residual analysis

INTRODUCTION

Centrifugal pumps are popular tools that are often used to move fluids in industries. In a centrifugal pump, kinetic energy is converted into pressure. Rotary mechanics are movements that occur in centrifugal pumps. The motion relies on the rotation around a central point to generate hydrokinetic energy to move the liquid. In general, centrifugal pumps are used in the food industry, wastewater treatment plants, agriculture, the oil and gas industry, and the paper and pulp industry [1]. Damage that can interfere with the performance and reliability of the pump will harm those industries. Fault detection and diagnosis systems are very important for overcoming these problems. Early detection of faults can help avoid product breakdowns, performance degradation, damage to machines, losses to human health, and even death [2]. Scholars have often conducted studies on pump fault detection. Various approaches or methods are used; some are model-based or data-based. Model-based methods generally rely on a mathematical model of the process derived from the system identification process. However, data-based methods rely only on process measurements to diagnose faults [3]. Data-based detection systems can be carried out in several ways, such as the fast Fourier transform [4], wavelet transforms [5] from vibration transmission, convolutional neural networks [6], and adaptive resonance theory neural networks [7].

The model-based detection system uses the principle of residual analysis. The residual is the signal generated from the difference between the model output and the measurement output. In general, the difference between researchers lies only in the method of obtaining the residuals and the residual analysis technique used. As in [8], the algorithm used for fault detection is a combination of structural analysis, observers, and analytical redundancy relations. In [9], the researcher used a fault diagnosis using the parity equation to generate the residuals. Residual analysis techniques can be performed in the time domain, as in [10], and frequency, as in [11]. Based on previous fault detection research, the model-based method has several advantages over the data-based method. For example, some of the advantages are high sensitivity to fault, robustness to modeling uncertainty, good attenuation of disturbance and noise, and the ability to distinguish simultaneous faults [12].

Model-based methods generally generate residuals using an observer, parameter estimation, and parity space, which require knowledge of plant dynamics through basic laws. However, under real conditions, there is no accurate mathematical model that can be obtained from non-linear systems. In addition, it is difficult to obtain a dynamic model of a plant with high nonlinearity. One solution to overcome this problem is to use an artificial neural network (ANN) based model. ANN is currently attracting the attention of researchers owing to their ability to study complex non-linear functions [13]. In addition, ANN can also identify non-linear models quickly and flexibly [14].

Therefore, in this study, we designed a pump fault detection system based on the residuals of ANN models. The residual analysis uses features in the time domain. As a case study, this study reviewed two centrifugal pumps that work for water flow, namely the water injection pump (WIP) and low-pressure oil flow, namely the medium-pressure oil pump (MPOP). One of the benefits offered by this proposed scheme is the use of the measurement results of process variables that already exist in the control room; therefore, there is no need to add a new measurement module. In addition, the

*CORRESPONDING AUTHOR | Katherin Indriawati | ✉ katherin@ep.its.ac.id

considered faults include those in the pumping system and not only in the pump. Furthermore, a condition monitoring scheme is discussed to detect faults online. This scheme was tested via a simulation.

CENTRIFUGAL PUMP

A pump is a tool that is useful for moving fluids by using a mechanical mechanism. A centrifugal pump is a kinetic machine that converts mechanical energy into fluid energy using centrifugal force [15]. The centrifugal pump has two main components: the rotating component consists of an impeller and a shaft, and the stationary component consists of a casing, casing cover, and bearing. The pumping system is illustrated in Figure 1. As the driving element, the motor converts electrical energy (in the form of current i) into mechanical energy (in the form of torque M). Thus, the mechanical part of the pump is rotated at speed ω. Then, the rotation causes an increase in the momentum of the pump fluid from the rotor inlet with a smaller radius to the rotor outlet with a larger radius and has the same value as the differential pressure Δp of the two inlet-outlet lines. The pump is connected to a piping system that transports a certain fluid at a flow rate Q that depends on the differential pressure of the pump. The input-output relationship of each block has very high nonlinearity [16].

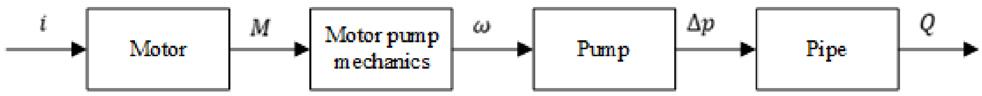

Figure 1. Pumping system block diagram

This study examines the types of pump faults that include suction blockage and cavitation syndrome on MPOP, and dirty suction strainers and pressure transmitter faults on the WIP. A dirty or clogged suction strainer can increase vibration/noise levels, insufficient suction or discharge pressure, cavitation, and poor pump efficiency [16]. Meanwhile, a fault in the pressure transmitter can cause an error in the measurement of process variables.

Cavitation is the phenomenon of vapor bubble formation owing to liquid evaporation as a result of the static pressure dropping below the vapor pressure of the fluid in the pump. Pressure shock from the burst of steam bubbles can destroy the pump over time. Cavitation can increase pump noise and vibration, as well as damage components, such as impeller erosion and mechanical seal damage. If this condition is severe, cavitation can break the shaft.

ANN RESIDUAL OF CENTRIFUGAL PUMP

The residual is the difference between the observed signal value and the estimated signal [17]. In this study, the residual refers to the difference in the output estimate value of the ANN model with the measurement value, hereafter referred to as the ANN residual. These residual values can be used to identify the condition of the pump system, whether it is in a normal condition or in the presence of a fault. For this reason, a residual analysis in the time domain was carried out, as described in the next section.

There are two measurement signals that are compared with the estimated signal from the ANN; the pressure difference between the suction and discharge lines, and the flow rate at the pump outflow. Based on the working principle of the pumping system, there are three ANN models, static, dynamic, and dynamic pump-pipe models, as shown in Figure 2. Thus, three residuals were generated: the residual of the differential pressure (r_1), pipe flow rate (r_2), and pump-pipe flow rate (r_3). The input and output of the artificial neural network model are based on research in [18] and are listed in Table 1.

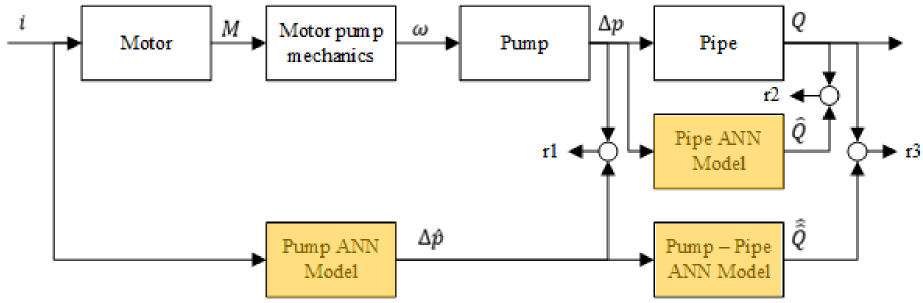

Figure 2. Residual analysis on centrifugal pump fault detection system

Table 1. Input-output variables of the ANN model

Model	Input	Output
Static pump	Measured current	Differential pressure estimate
Dynamic pump	Measured differential pressure	Pump flowrate estimate
Dynamic pump-pipe	Differential pressure estimate	Pump-pipe flowrate estimate

Note that even though the quantity that enters the dynamic models is the same, namely, differential pressure, the origin of the data is different. The differential pressure signal that enters the dynamic pump model is derived from the measurement results, whereas the signal that enters the dynamic pump-pipe model is derived from the estimation results. Based on historical maintenance data, the process data are grouped into normal and fault condition data. The ANN model used normal-condition data for training and model validation. However, it is necessary to conduct data pre-processing first to clean data from outliers because outliers are assumed to be reading errors. Some of the data deviated very highly, and some deviated very poorly. Cleaning is performed on outliers that deviate very far from most other data, so that the input-output data pair is truly representative of the existing conditions.

In this study, ANN modeling uses a feedforward architecture consisting of three layers (one input layer, one hidden layer, and one output layer), as shown in Figure 3(a). An ANN structure with one input neuron functions as a Simple Linear Regression (SLR), which is fitted with a straight line on only one predictor with the criteria of the least-squares method [19]. In addition, related to hidden neurons in the hidden layer, Guliyev et al. explained that a feedforward network with only one neuron in the hidden layer could still estimate the continuous function arbitrarily [20]. The use of one hidden neuron was also carried out in the study of Zhang et al., where the performance of the artificial neural network model with one hidden neuron was sufficiently good [21]. The output of the ANN model y described on Figure 3(b) was computed using the following equation:

$$y = f\left(\sum_{j=1}^{N} w_j z_j + b\right) \tag{1}$$

where z_j is the j^{th} input value, w_j is the corresponding weight value, b is the bias term, N is the number of hidden neurons and f is the activation function. The activation function can be logarithmic sigmoid or linear.

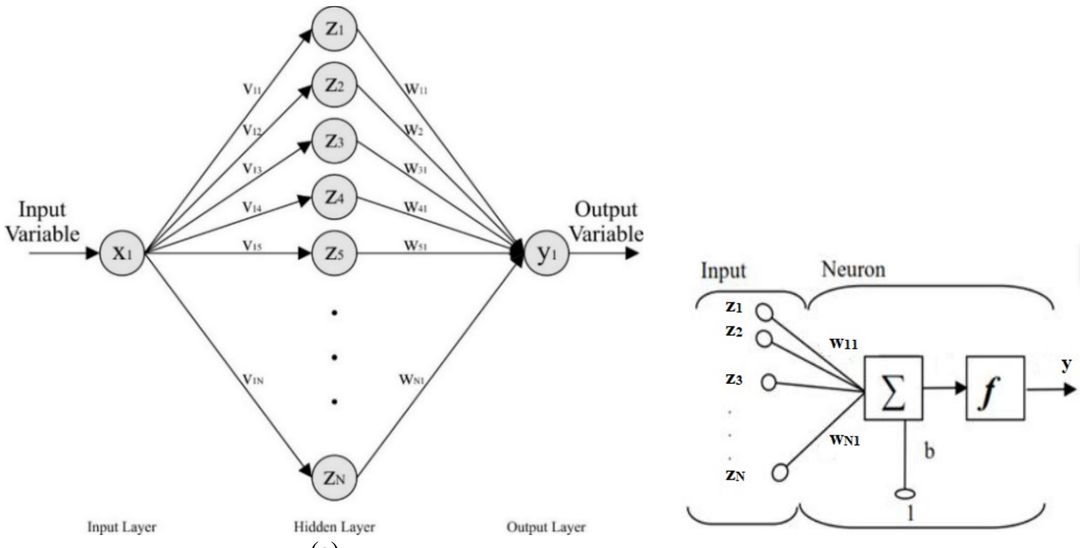

Figure 3. (a) ANN model structure and (b) a neuron in the output layer

In this study, the artificial neural network architecture was designed using the parameters listed in Table 2. Furthermore, researchers varied the number of neurons (nodes) to obtain the best performance of the artificial neural network architecture. Variations in the number of neurons were between 1-20 in the hidden layer.

The procedure used to modify the synaptic weights of the network in an orderly fashion to attain the desired design objective was backpropagation. This learning algorithm is most commonly used to train ANN. This is a supervised learning method that uses an error term (the difference between the desired and target values) to adjust the synaptic weights. This process was repeated until the mean square error (MSE) was reduced to an acceptably low value.

The first stage in determining the weight of the ANN is data normalization, which aims to change the value of the original process variable to the value of the process variable within a range of 0–1. It aims to make the artificial neural network able to learn well. Data normalization was performed using the following equation:

$$x' = \frac{x-b}{a-b} \tag{2}$$

where x’ is the normalized data, x is the original data, a is the maximum value of the original data, and b is the minimum value of the original data. The next stage involved training and validation. The training phase was conducted by using the parameters listed in Table 2. The number of hidden neurons in the hidden layer was then determined by varying the number of hidden neurons from 1 to 20. Subsequently, the researchers used the architecture that provided the best performance.

Table 2. Parameters of artificial neural network architecture design

Parameters	Information
Network type	Feedforward backpropagation
Training algorithm	Levenberg-Marquardt
Performance function	Mean square error (MSE)
Epoch maximum	1000
Number of layers	3 (1 input layer, 1 hidden layer, 1 output layer)
Number of neuron	Variation 1 – 20
Activation function	Hidden layer by using LOGSIG Output layer by using PURELIN
Data composition	*MPOP* Training: 2198 data (74,99%) Validation: 733 data (25,01%) *WIP* Training: 1360 data (80%) Validation: 340 data (20%)

The best architecture was obtained from the smallest root mean square error (RMSE) and mean absolute percentage error (MAPE) values. Smaller RMSE and MAPE values indicate that the architecture can produce an output with a small error compared to other architectures. RMSE and MAPE can be expressed as follows:

$$RMSE = \sqrt{\frac{\Sigma(y_i - \hat{y}_i)^2}{n}} \tag{3}$$

$$MAPE = \frac{1}{n}\sum_{i=1}^{n}\left|\frac{y_i - \hat{y}_i}{\hat{y}_i}\right| \times 100\% \tag{4}$$

where y_i is the i^{th} target value, $\hat{y}_i$ is the i^{th} output value of the neural network, and n is the amount of output data.

RESIDUAL-BASED DETECTION SYSTEM

A block diagram of a fault detection system that uses residuals to perform fault detection and diagnosis is shown in Figure 4.

Residual Ensemble Generation

Residual generation was conducted by calculating the difference between the X_P pump process variable signal and the ANN model output signal, X_M, when the same U input was used. Moreover, the process data are arranged in the form of ensembles, which are collections of cells containing several process variable values. In this study, there are three ensembles, each of which represents the condition of the pump, namely, one ensemble for healthy and two ensembles for faults. Each ensemble contained 40 data cells, where each cell contained two process variable values, namely differential pressure and flow rate. Each cell has 25 data. Next, this ensemble was used to produce a residual ensemble.

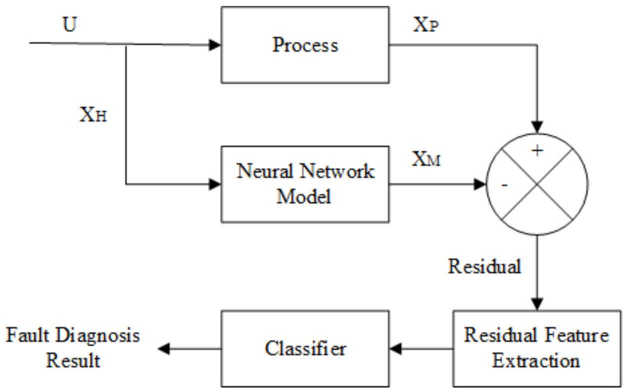

Figure 4. Block diagram of the proposed fault detection system

The residual ensemble dimensions were consistent with the data ensemble dimensions, with a matrix of 40 × 3 dimensions derived from 40 rows of cell data and three columns of residual types. Based on the three ANN models in Table 1, three types of residuals are generated in each pump condition: residuals from model 1 (r_1), residuals from model 2 (r_2), and residuals from model 3 (r_3).

Residual Feature Extraction

After the residuals were generated, feature extraction was performed from the three types of residuals. Feature extraction is computationally specific and can characterize signals [22]. The residual feature used in this study is a statistical parameter of the residual signal, which is the value in [23].

a) Mean: the average value of the overall residual value, written as follows:

$$\bar{x} = \frac{\sum_{i=1}^{n} x_i}{n} \tag{4}$$

where $\bar{x}$ is the mean residual value, x_i is the i^{th} residual value, and n is the amount of residual data.

b) Max: The maximum value of the entire residual or is written as follows:

$$x_{peak} = \max |x_i| \tag{5}$$

c) Kurtosis: This is an indicator that shows the level of sharpness of the data, where the greater the kurtosis value, the sharper the shape of the distribution curve. This is based on the following equation:

$$x_k = \frac{\sum_{i=1}^{n}(x_i - \bar{x})^4}{(n-1)x_{sd}^4} \tag{6}$$

where x_k is the kurtosis value, and x_{sd} is standard deviation.

d) Variance: how far a residual value deviates from its average value, calculated by the following equation:

$$x_v = x_{sd}^2 = \frac{\sum_{i=1}^{n}(x_i - \bar{x})^2}{n-1} \tag{7}$$

e) One-Norm: is the sum of the residuals absolute values.

$$|x|_1 = \sum_{i=1}^{n} |x_i| \tag{8}$$

Thus, for the three residuals reviewed in this study, there were 15 features. For example, for residual r_1 there are Mean1, Max1, Variance1, Kurtosis1, and OneNorm1 features, as shown in Table 3.

Table 3. Residual feature codes

Feature type	Residual of		
	Static pump model	Dynamic pump model	Dynamic pump-pipe model
Mean	Mean1	Mean2	Mean3
Maximum	Max1	Max2	Max3
Kurtosis	Kurtosis1	Kurtosis2	Kurtosis3
Variance	Variance1	Variance2	Variance3
One-norm	OneNorm1	OneNorm2	OneNorm3

Residual Feature Classifier

In machine learning, a classifier is an algorithm that can automatically categorize data into classes or labels. The classifier identifies the appropriate class, type, or category based on observed data. The classifier works by training a model with a training dataset, and the resulting model is used to predict the class in a set of data tests. Four types of classifiers were used in this study: support vector machines, decision tree, naïve Bayes, and K – Nearest neighbor. Next, the researcher used the residual feature input obtained from the previous stage. The residual feature classifier data consisted of statistical parameters (see Table 3) and pump condition labels: normal, fault-1 (suction blockage on MPOP/dirty suction strainer on WIP), and fault-2 (cavitation syndrome on MPOP/pressure transmitter fault on WIP). Thus, overall, 45 data types are used in designing the classifier for one centrifugal pump (WIP or MPOP).

In the classifier design, there are two stages: training and validation. Therefore, the residual feature data were divided into two parts: 80% for training and 20% for testing. Only the classifier with the best performance was selected and used in the detection-system testing phase. The parameters used to measure the performance of the classifier were accuracy, precision, and recall. The classifier performance can be described as follows [24].

i. Precision is a parameter that provides an estimate of how often the prediction results show the actual conditions.

$$Precision = \frac{TP}{TP + FP} \tag{9}$$

ii. Recall: This parameter describes how often the condition data can be detected by the classifier from the training results.

$$Recall = \frac{TP}{TP + FN} \tag{10}$$

iii. Accuracy: a parameter that defines how well the classifier can distinguish classes.

$$Accuracy = \frac{TP + TN}{TP + TN + FP + FN} \tag{11}$$

where true positives (TP) and true negatives (TN) are the outcomes of the positive and negative classes, respectively, correctly classified by the model, whereas false positives (FP) and false negatives (FN) are incorrectly classified outcomes.

Design of Online Monitoring

In this study, the detection system generated for each pump type was applied to an online monitoring scheme. A schematic of the pump condition monitoring system is shown in Figure 5. The input of this system consists of the measured current, flow rate, and differential pressure, whereas the output is the label of the predicted fault. The measured variables were obtained online using the data acquisition system.

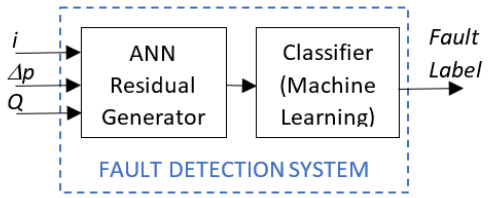

Figure 5. Pump condition monitoring system

To determine the performance of the online condition monitoring system, this system was tested by simulation, the scheme of which is shown in Figure 6. Dynamic data from the process variable simulation (testX), which consists of the measured current, flow rate, and differential pressure, are fed to the prediction function block as the proposed fault detection system so that it can predict the pump condition (class label). Next, the prediction results are compared with the actual conditions (test Y) such that the correct prediction value can be calculated in the form of Boolean logic data. The data were then entered into the accuracy function block to calculate the level of prediction accuracy.

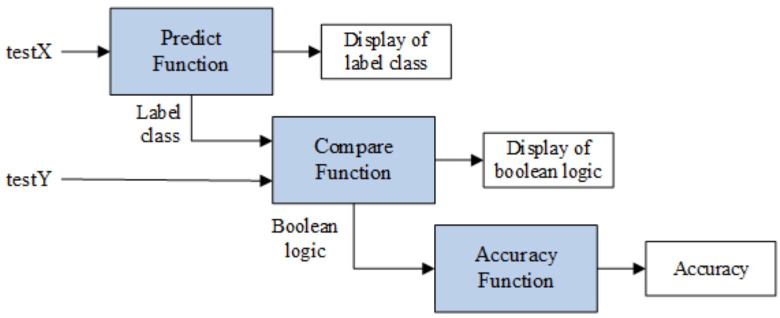

Figure 6. Testing scheme of the proposed online system

RESULTS AND DISCUSSION

The specifications of the MPOP and WIP used as the research objects are listed in Table 4. Both are pump units in PT. Saka Indonesia Pangkah Limited, which is equipped with a Piping and Instrumentation Diagram (P&ID), as shown in Figure 7. In addition to the differences in fluid usage, the difference between the MPOP and WIP also lies in the capacity and power of the pump.

Table 4. Review of centrifugal pump specifications

Parameters	MPOP	WIP
Liquid type	Oil	Produced water
Rated flowrate	110 m^3/h	213 m^3/h
Suction pressure	22,5 barg	15,5 barg
Discharge pressure	71,43 barg	97,2 barg
Differential pressure	45,93 bar	81,7 bar
Differential head	632 m	838,9 m
Temperature	40,3 ºC	40 ºC
Impeller type	Closed	Closed
Driver type	Induction motor	Induction motor
Rated of speed	2967 rpm	2969 rpm

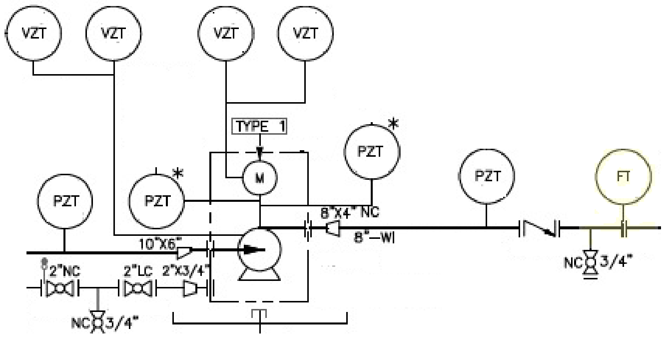

Figure 7. The P&ID of the installed pumps

The data used in this study include operation (process) and maintenance data. The operation data are historical data from the three units of WIP and MPOP. The historical data used included normal pump data and faulty pump data. Thus, the initial stage of the experiment was to sort the normal pump data and fault-condition pump data. The next stage was pre-processing to remove outliers. The results of this stage are data that are ready to be used in designing the proposed detection system through the following stages: modeling normal pump conditions using the neural network method, generating residuals, extracting residual features with a statistical approach, and constructing a proper classifier. Finally, the proposed detection system design results were implemented in an online monitoring scheme. The experimental procedure is shown in the flowchart of Figure 8.

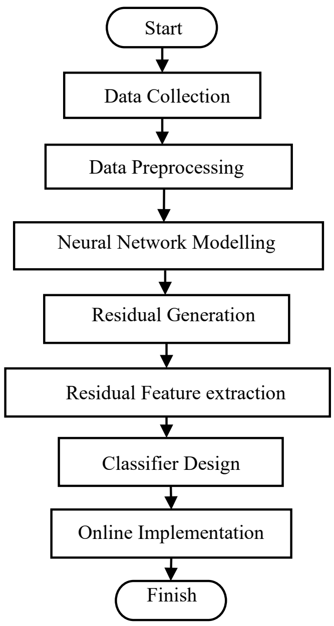

Figure 8. The flowchart of the overall methodology

Residual Generation

The operation data consist of several process variables, such as current, flow rate, suction, and discharge pressure, which can be accessed in the control room. Thus, the related sensors were located in the pump motor for current measurement, in the pump outlet for flow rate and discharge pressure measurements, and in the pump inlet for suction discharge measurement. The differential pressure variable was obtained from the difference between the discharge and suction pressure. Furthermore, historical maintenance data includes the type of fault and action taken.

Based on the training and validation results, the best ANN model was obtained with the number of hidden neurons, as shown in Table 5, and the validation results are shown in Table 6. Based on the validation results, it can be seen that the largest RMSE value is in the dynamic pump-pipe model of the WIP pump. This is because the input of this model is not from the measurement results but from the estimation results of the static pump model; there is a double error. However, the dynamic pump-pipe model of an artificial neural network exhibits the expected performance. Based on the MAPE value, the entire design of the MPOP and WIP pump-estimation models had a value of less than 10%. This means that the prediction results are included in the high-accuracy category; therefore, the model is valid for representing the healthy condition of the pump.

Table 5. The number of hidden neurons with the best performance

Model	Number of hidden neuron	
	MPOP	WIP
Static pump	1	1
Dynamic pump	17	1
Dynamic pump – pipe	2	1

Table 6. ANN model validation results

Model	MPOP		WIP	
	RMSE	MAPE	RMSE	MAPE
Static pump	0.0174	2.5547	1.0940	0.95546
Dynamic pump	0.0461	8.8969	1.0044	0.43213
Dynamic pump - pipe	0.0450	7.4179	5.4540	2.23170

The validation results are also shown using a comparison graph of the ANN model output (blue circle) and the measured value as the target (red circle), as shown in Figure 9 for the WIP case. There are several estimates with results that have a small difference from the target. In addition, some estimates do not meet the target. However, this occurs in outlier data. The results of the artificial neural network-based modeling from the previous stage were used to generate the residual signals. Based on the model, each pump condition, both healthy and faulty, had three types of residuals. The residual stored the condition characteristics of the pump. The residual signal is shown in Figure 10. In this case, 25 residual data points are obtained.

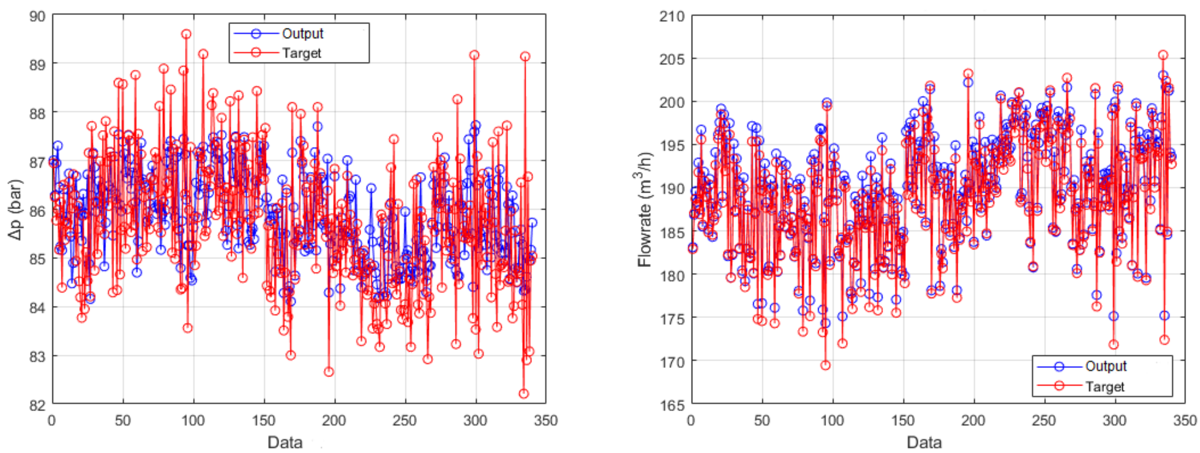

(a) static pump model (b) dynamic pump model

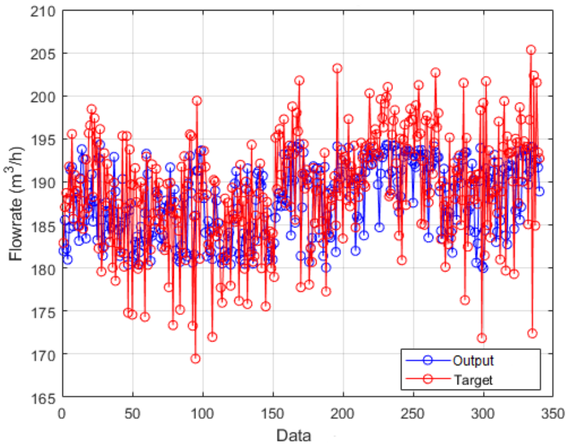

(c) dynamic pump–pipe model

Figure 9. WIP model validation

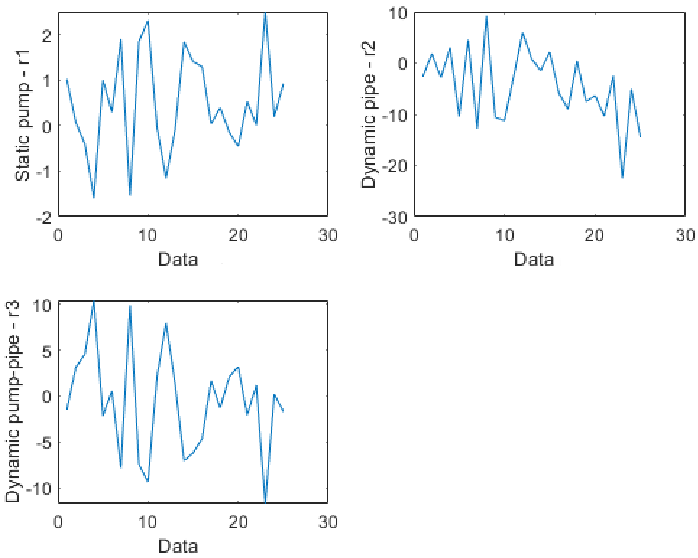

Figure 10. Residual plot for WIP case

Residual Feature Extraction Results

The relationship between certain residual features for the healthy (blue) and fault (red and green) conditions is shown in Figure 11 for the MPOP and Figure 12 for the WIP. The graph shows the distribution of each feature in the diagonal position. Meanwhile, in nondiagonal positions, there are plots of two residual feature values.

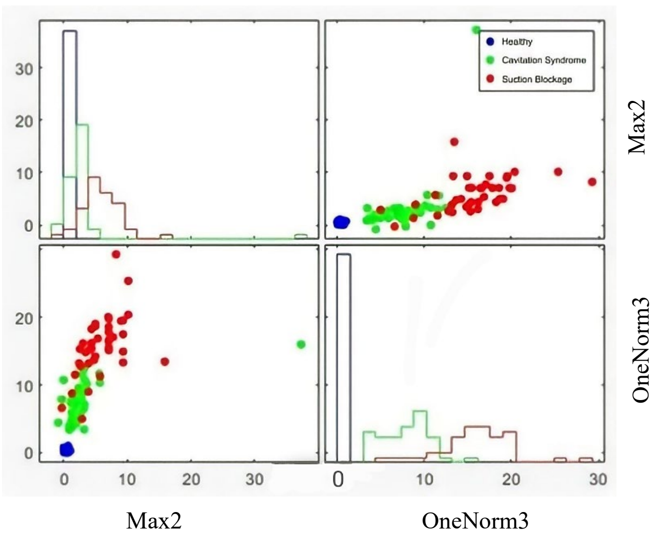

Figure 11. Max2 and OneNorm3 features on MPOP

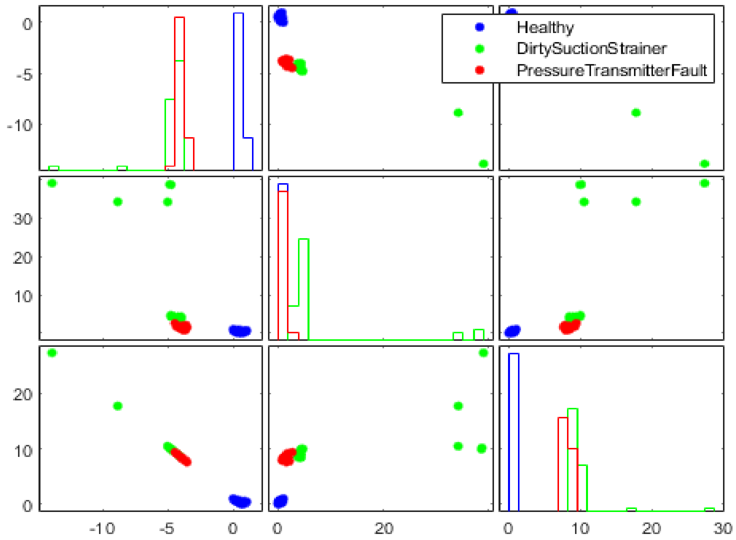

Figure 12. Mean2, Max1, and OneNorm2 features on WIP

For example, in Figure 11, the first column and first row are Max2 distribution graphs, whereas the second column and second row are OneNorm3 distribution graphs. On the other hand, the graph of the relationship between Max2 and OneNorm3 is shown in the first column – second line and second column – second row. In Figure 12, there are nine graphs, namely Mean2, Max1, and OneNorm2, because three residual features are considered. Fault can be distinguished based on the scatter plot. This is because some residual features have a fairly well-separated distribution of data between normal and fault conditions. However, some data were still close to the fault condition. In addition, not all residual features have good data separability; therefore, they were analyzed manually using a scatter plot. Moreover, if there are many fault analyses, the possibility of faults identification increases. Therefore, in this study, machine learning was used to classify the fault types automatically.

Residual Feature Classifier Results

The next stage is the design of multi-classification based on machine learning using Support Vector Machines (SVM), Gaussian Naïve Bayes (GNB), and K-Nearest Neighbors (KNN) methods. A comparison of the training results of the two best methods is presented in Table 7 for MPOP and Table 8 for WIP. Thus, SVM was selected as the classifier for MPOP, whereas GNB was selected as the classifier for WIP. A precision value of 100% was obtained under healthy conditions.

Table 7. Comparison of training classifier performance under MPOP conditions

Condition	Parameter (%)					
	Precision		Recall		Accuracy	
	SVM	KNN	SVM	KNN	SVM	KNN
Healthy	100	100	100	100		
Cavitation syndrome	96.87	93.75	86.11	85.71	93.75	92.71
Suction blockage	84.37	84.37	96.43	93.10		

Table 8. Comparison of training classifier performance in WIP conditions

Condition	Parameter (%)					
	Precision		Recall		Accuracy	
	GNB	KNN	GNB	KNN	GNB	KNN
Healthy	100	100	100	100		
Dirty suction strainer	100	90.6	84.4	90.6	94.8	93.8
Pressure transmitter fault	86.5	90.6	100	90.6		

At the MPOP testing stage, the SVM classifier performed well in detecting the centrifugal pump condition, as shown in the confusion matrix in Figure 13. Meanwhile, for the suction blockage condition, the SVM classifier was able to detect six of the eight conditions correctly, where two data were read incorrectly as a condition of cavitation syndrome, so the precision value of the suction blockage category was only 75% (Table 9). This is referred to as a false negative, which is a condition when the actual condition data are detected as another condition data. System detection faults can occur because the statistical feature values in each condition are almost the same. In this case, cavitation syndrome and suction blockage have similar features. For the recall performance parameter in the testing phase, the SVM classifier has a value of 100% for healthy conditions and suction blockage and 80% for cavitation syndrome conditions.

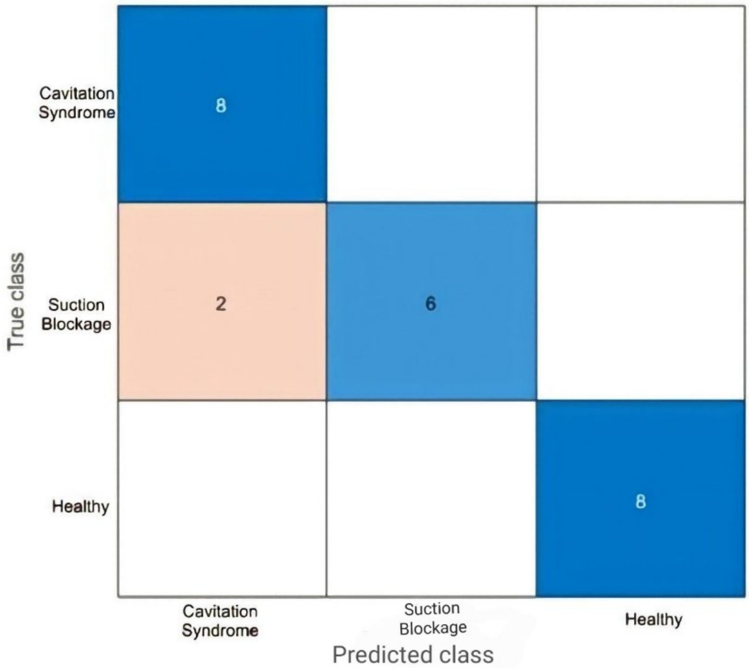

Figure 13. Confusion matrix with Support Vector Machine classifier testing

Table 9. Support Vector Machine classifier performance parameters

Condition	Parameter (%)					
	Precision		Recall		Accuracy	
	Train	Test	Train	Test	Train	Test
Healthy	100	100	100	100		
Cavitation syndrome	96.87	100	86.11	80	93.75	91.67
Suction blockage	84.37	75	96.43	100		

In the WIP case test, the GNB classifier produced a confusion matrix, as shown in Figure 14. For fault conditions, GNB correctly detected seven of the eight conditions. Based on the test performance in Table 10, the prediction accuracy of the test data is 91.67%. The sensitivity (recall) of the healthy class was higher than that of the fault class. This is because one data point from each fault is incorrectly predicted as another type of fault. In this case, the transmitter fault condition and suction fault have features with similar values (see Figure 10, red and green coincide). When referring to the values of precision and recall, GNB produces 100% correct predictions for healthy conditions and 87.5% for fault conditions.

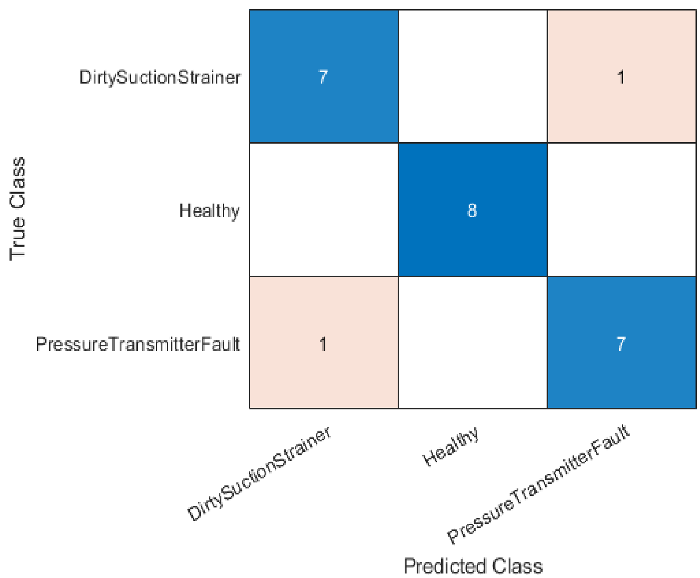

Figure 14. Confusion matrix Gaussian Naïve Bayes classifier testing

Table 10. Gaussian Naive Bayes classifier performance parameters

Condition	Parameter (%)					
	Precision		Recall		Accuracy	
	Train	Test	Train	Test	Train	Test
Healthy	100	100	100	100		
Dirty suction strainer	100	87.5	84.4	87.5	94.8	91.67
Pressure transmitter fault	86.5	87.5	100	87.5		

Online Monitoring

The results of the online monitoring simulation are shown in Figure 15 (a) for MPOP and Figure 15 (b) for WIP. Based on the results of the online monitoring simulation, it can be seen that the system has been able to detect faults with an accuracy of 99.43% for MPOP and 100% for WIP. All test data were detected correctly under healthy conditions, cavitation syndrome, dirty suction strainer, and pressure transmitter fault. Detection faults occurred momentarily in the suction blockage condition, where 17 data were read as cavitation syndrome conditions (Figure 15 (left)). However, the fault detection system that has been developed can detect changes in the steady state of the pump from healthy to fault according to the test data entered in general.

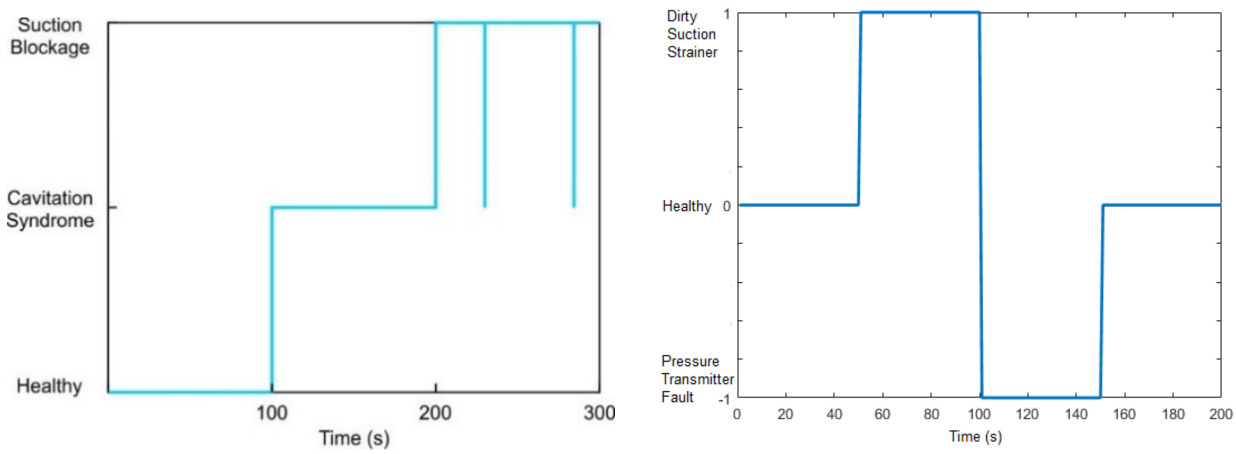

(a) MPOP (b) WIP

Figure 15. Condition monitoring results

CONCLUSIONS

The ANN-based fault detection strategy proposed in this study has been proven to be able to detect healthy conditions and fault conditions in centrifugal pumps with 100% accuracy. Meanwhile, the accuracy reached 91% for fault diagnosis purposes. In addition, this system can detect changes in pump conditions with an accuracy rate of > 99% when used for online monitoring purposes. The use of ANN has proven to be a good alternative for the residual estimation of complex plants with parameters that depend on operating conditions. Therefore, a fault database must be available such that the detection system can work for various types of faults. This is a novelty for further research.

ACKNOWLEDGEMENT

The authors are grateful to the Institut Teknologi Sepuluh Nopember for their financial support under the Publication Writing and IPR Incentive Program (PPHKI) project scheme.

REFERENCES

[1] N. R. Sakthivel, V. Sugumaran, and S. Babudevasenapati, "Vibration based fault diagnosis of monoblock centrifugal pump using decision tree," *Expert Systems with Applications*, vol. 37, no. 6, pp. 4040–4049, 2010.

[2] J. Gertler, *Fault detection and diagnosis in engineering systems*, Boca Raton: CRC Press, 1998.

[3] M. S. Mahmoud and H. M. Khalid, "Expectation maximization approach to data-based fault diagnostics," *Information Sciences (Ny)*., vol. 235, pp. 80–96, 2013.

[4] D. Siano and M. A. Panza, "Diagnostic method by using vibration analysis for pump fault detection," *Energy Procedia*, vol. 148, pp. 10–17, 2018.

[5] B. Kamiel, K. Mckee, R. Entwistle, I. Mazhar, and I. M. Howard, "Multi fault diagnosis of the centrifugal pump using the wavelet transform and principal component analysis," *Mechanisms and Machine Science*, vol. 21, pp. 555–566, Jan. 2015.

[6] Y. H. Eom, J. W. Yoo, S. Bin Hong, and M. S. Kim, "Refrigerant charge fault detection method of air source heat pump system using convolutional neural network for energy saving," *energy*, vol. 187, p. 115877, 2019.

[7] Z. Li, Z. Ma, Y. Liu, W. Teng, and R. Jiang, “Crack fault detection for a gearbox using discrete wavelet transform and an adaptive resonance theory neural network,” *Strojniski Vestnik*, vol. 61, pp. 63–73, Jan. 2015.

[8] C. S. Kallesoe, V. Cocquempot, and R. Izadi-Zamanabadi, “Model based fault detection in a centrifugal pump application,” *IEEE Transactions on Control Systems Technology*, vol. 14, no. 2, pp. 204–215, 2006.

[9] R. Isermann, “Model-based fault-detection and diagnosis – status and applications,” *Annual Reviews in Control,* vol. 29, no. 1, pp. 71–85, 2005.

[10] P. Samanipour, J. Poshtan, and H. Sadeghi, “Cavitation detection in centrifugal pumps using pressure time-domain features,” *Turkish Journal of Electrical Engineering & Computer Sciences,* vol. 25, pp. 4287–4298, Jan. 2017.

[11] M. A. S. ALTobi, G. Bevan, P. Wallace, D. Harrison, and K. P. Ramachandran, “Centrifugal pump condition monitoring and diagnosis using frequency domain analysis,” in *Advances in Condition Monitoring of Machinery in Non-Stationary Operations. CMMNO 2018: Applied Condition Monitoring,* A. Fernandez Del Rincon, F. Viadero Rueda, F. Chaari, R. Zimroz, M. Haddar, Eds. Cham: Springer, 2019, pp. 122-131.

[12] P. Freeman, R. Pandita, N. Srivastava, and G. J. Balas, “Model-based and data-driven fault detection performance for a small UAV,” *IEEE/ASME Transactions on Mechatronics*, vol. 18, no. 4, pp. 1300–1309, 2013.

[13] P. Subbaraj and B. Kannapiran, “Artificial neural network approach for fault detection in pneumatic valve in cooler water spray system,” *International Journal of Computer Applications*, vol. 9, no. 7, pp. 43–52, 2010.

[14] F. Kimmich, A. Schwarte, and R. Isermann, “Fault detection for modern Diesel engines using signal- and process model-based methods,” *Control Engineering Practice*, vol. 13, no. 2, pp. 189–203, 2005.

[15] Sularso and T. Haruo, *Pompa dan Kompresor*. Jakarta: PT. Pradya Paramita, 2000.

[16] J. Raza, J. P. Liyanage, H. Al Atat, and J. Lee, “A comparative study of maintenance data classification based on neural networks, logistic regression and support vector machines,” *Journal of Quality in Maintenance Engineering,* vol. 16, no. 3, pp. 303–318, Jan. 2010.

[17] I. Fagarasan and S. S. Iliescu, “Parity equations for fault detection and isolation,” in 2008 IEEE International Conference on Automation, Quality and Testing, Robotics, 2008, vol. 1, pp. 99–103.

[18] R. Isermann, *Fault-Diagnosis Applications*. Berlin Heidelberg: Springer, 2011.

[19] T. D. Parsons, A. A. Rizzo, and J. G. Buckwalter, “Backpropagation and regression: comparative utility for neuropsychologists,” *Journal of Clinical and Experimental Neuropsychology*, vol. 26, no. 1, pp. 95–104, Jan. 2004.

[20] N. J. Guliyev and V. E. Ismailov, “A single hidden layer feedforward network with only one neuron in the hidden layer can approximate any univariate function,” *Neural Computation,* vol. 28, no. 7, pp. 1289–1304, 2016.

[21] C.-L. Zhang, “Generalized correlation of refrigerant mass flow rate through adiabatic capillary tubes using artificial neural network,” *International Journal of Refrigeration,* vol. 28, no. 4, pp. 506–514, 2005.

[22] V. Muralidharan, V. Sugumaran, P. Shanmugam, and K. Sivanathan, “Artificial neural network based classification for monoblock centrifugal pump using wavelet analysis,” *International Journal of Mechanical Engineering and Technology*, vol. 1, pp. 28–37, 2010.

[23] E. Sayed, A. A. Abdelsamee, and N. M. Ghazaly, “Classification model using neural network for centrifugal pump fault detection,” *International Journal of Systems Signal Control and Engineering Application*, vol. 13, no. 4, pp. 120-126, 2020.

[24] S. K. Venkata and S. Rao, “Fault detection of a flow control valve using vibration analysis and support vector machine,” *Electronics* , vol. 8, no. 10. 2019.